

## 4.7 THE INFLUENCE OF IMPROVED LAND SURFACE AND SOIL DATA ON MESOSCALE MODEL PREDICTIONS

Christopher M. Godfrey\*  
University of Oklahoma, Norman, Oklahoma

David J. Stensrud  
NOAA National Severe Storms Laboratory, Norman, Oklahoma

Lance M. Leslie  
University of Oklahoma, Norman, Oklahoma

### 1. INTRODUCTION

Land surface characteristics play a critical role in the evolution of the planetary boundary layer of the atmosphere. Several key components of the land surface that significantly affect surface sensible heat and moisture fluxes include soil temperature and moisture, fractional vegetation coverage ( $\sigma_f$ ), and green leaf area index (LAI). The lack of observational data for accurate specification of these components in model initial conditions is one of the most difficult aspects in the evaluation of land surface models. Soil temperature and moisture measurements are unavailable in most areas and routine observations of  $\sigma_f$  and LAI are not available at high resolution, i.e., with pixel widths on the order of 1 km and daily updates. This gap in our observational capabilities seriously hampers the evaluation and improvement of land surface model parameterizations, since it is very likely that model errors are related to improper initial conditions as much as to inaccuracies in the model formulations.

The Penn State–National Center for Atmospheric Research fifth-generation Mesoscale Model (MM5) version 3 (Dudhia 1993; Grell et al. 1994) implements a monthly climatology for fractional vegetation coverage and a constant leaf area index (LAI). Studies have shown that such coarse resolution data based solely on climatology are insufficient to capture the detailed surface characteristics necessary to properly initialize a land surface parameterization (e.g., Chang and Wetzel 1991; Crawford et al. 2001; Kurkowski et al. 2003). By using climatological values for land surface characteristics, the model does not account for short-term or annual variability in vegetation coverage and condition due to daily variations in rainfall, seasonal droughts, flooding, forest fires, irrigation, deforestation, desertification, crop harvesting, land usage, hail or tornado damage, and temporal variations in the growth and senescence of green vegetation. Modeling studies implementing near real-time land surface characteristics from satellite observations have shown great promise for improving forecasts (e.g., Crawford et

al. 2001; Kurkowski et al. 2003; Oleson and Bonan 2000; Zeng et al. 2000).

Proper specification of initial soil moisture and temperature is also imperative for land surface models to accurately forecast surface variables (Crawford et al. 2000). Soil moisture affects runoff and is important in regulating the interchange between latent heat flux and sensible heat flux. Without accurate soil information, the planetary boundary layer scheme may incorrectly distribute heat near the surface. Substrate temperatures may be too cold or warm, leading to a cooling or warming bias at the surface (Dudhia 1996).

In an effort to improve the specification of initial conditions, and to ultimately facilitate improved model forecasts, a modified version of MM5 ingested near real-time  $\sigma_f$  and LAI fields at 1-km resolution. These vegetation indices originated from daily updates of National Oceanic and Atmospheric Administration (NOAA) Advanced Very High Resolution Radiometer (AVHRR) normalized difference vegetation index (NDVI) data. The model also incorporated real-time soil temperature and moisture measurements from the Oklahoma Mesonet. In addition to supplying initial soil conditions, this dense network of surface observations over the primary study area provided a means to verify MM5 forecasts and to assess the influence of improved surface initial conditions in a land surface model. The following sections discuss the origin of additional land surface data and the procedure for assimilating those data into the model, illustrate a comparison of several key surface variables for different model forecasts, discuss the impact of improved initial conditions on model forecasts, and discuss implications for further data requirements.

### 2. DATA

#### 2.1 Oklahoma Mesonet

The Oklahoma Mesonet is a network of automated surface observing stations, with at least one site in each of Oklahoma's seventy-seven counties. Measurements of atmospheric variables occur every five minutes at each of the 116 sites. All sites measure soil temperature every fifteen minutes at a depth of 10 cm under both bare soil and native vegetation. Approximately half of the sites measure soil temperature at a depth of 5 cm under both

---

\*Corresponding author address: Christopher M. Godfrey, University of Oklahoma, School of Meteorology, 100 E. Boyd Street, Suite 1310, Norman, Oklahoma 73019; e-mail: christopher.godfrey@noaa.gov.

bare soil and native vegetation and at a depth of 30 cm under native vegetation. Sixty sites also take readings every thirty minutes that can be converted into soil moisture values at levels of 5, 25, 60, and 75 cm below the surface. Seventy-five sites measure ground heat flux and total net radiation every five minutes. A special suite of instruments augments the standard instrumentation at ten sites, thereby measuring sensible and latent heat flux and the four components of net radiation every five minutes. All data fall subject to rigorous quality assurance procedures in order to produce reliable research-quality data (Shafer et al. 2000). A complete description of the Oklahoma Mesonet, including sensor specifications, appears in Brock et al. (1995), while Basara and Crawford (2000) describe the soil moisture instrumentation.

## 2.2 NOAA AVHRR satellites

The AVHRR subsystem resides aboard several NOAA Polar Orbiting Environmental Satellites (POES). Each flies at an altitude of  $833 \pm 19$  km in a sun-synchronous orbit with a period of  $101.6 \pm 0.5$  min. The local solar time of the satellite's passage is constant for any latitude. Thus, multiple images of the same location show the same sun angle, excepting changes in illumination over long time periods due to orbital drift (Kidwell 1998). Two primary satellites work in tandem to sample the entire planet daily, with several backup satellites available should a primary satellite fail. The AVHRR subsystem measures six spectral channels with a field of view of 1.3 milliradians by 1.3 milliradians, giving a ground resolution of 1.09 km. Details of the newest AVHRR/3 system appear in Goodrum et al. (2001).

Several types of vegetation indices derive from AVHRR data (e.g., Viña et al. 2004), but NDVI is the most popular vegetation index used to derive  $\sigma_f$  and LAI. NDVI is given by

$$\text{NDVI} = \frac{\rho_2 - \rho_1}{\rho_2 + \rho_1}, \quad (1)$$

where  $\rho_1$  and  $\rho_2$  are reflectance measurements by a silicon detector in AVHRR channels 1 ( $0.58\text{--}0.68 \mu\text{m}$ ) and 2 ( $0.725\text{--}1.00 \mu\text{m}$ ), respectively (Goodrum et al. 2001; Gutman and Ignatov 1998). The high reflectance of near-infrared light ( $\rho_2$ ) and the low reflectance of visible red light ( $\rho_1$ ) on vegetation produce larger values of NDVI. Conversely, the low reflectance of near-infrared light and high reflectance of red light from clouds, snow, water, and bare soil produce low (typically negative) values of NDVI (Zhangshi and Williams 1997). NDVI is useful because it partially compensates for changes in illumination, surface slope, and viewing angle, all of which strongly affect observed radiances (Gutman et al. 1995).

Traditionally, composite maximum NDVI images over a period of weeks are effective at eliminating low NDVI values due to cloud contamination and provide for appropriate parameterizations of vegetation coverage (e.g., Crawford et al. 2001; Kurkowski et al. 2003). The cur-

rent study employed a fifteen-day observation window for computing maximum NDVI composites.

The model grid cell fraction where midday downward solar radiation is intercepted by a photosynthetically active green canopy (Chen et al. 1996) defines  $\sigma_f$ . This acts as a weighting coefficient between direct evaporation from the top soil layer, evaporation of precipitation intercepted by the canopy layer, and transpiration from the vegetation. Depending on the season and the area of interest,  $\sigma_f$  could conceivably range from 0% to 100%. The ratio of total leaf area to its covered ground area (Zhangshi and Williams 1997) defines the LAI, which is a measure of the vegetation biomass. Typical values of LAI vary depending on the biome represented in a satellite pixel, but may have maxima between 6 and 8 for deciduous forests and between 2 and 4 for annual crops. Desert and tundra yield low LAI values near 0.1, while LAI for coniferous forests may exceed 15. Area-averaged LAI values such as those measured by satellite display lower maxima and a narrower range of values than point measurements (Scurlock et al. 2001).

Since NDVI is a function of both  $\sigma_f$  and LAI, Gutman and Ignatov (1998) concluded that both  $\sigma_f$  and LAI cannot be regarded as two independent pieces of information and should not be used together in the same land-surface parameterization. However, it is advantageous to provide the model with as much information as possible. The two vegetation indices are relatively independent within the land surface model selected for this study. LAI is used to calculate canopy resistance, while  $\sigma_f$  is used to calculate evaporation terms. Together, LAI and  $\sigma_f$  specify the total canopy evapotranspiration.

Errors introduced by the dual specification of vegetation parameters from a single NDVI observation are likely smaller than the inadequacies inherent in the model. For example, at 1-km resolution  $\sigma_f$  and LAI observations are smoothed in all but the smallest nested domain. In addition, Eta model analysis fields on a 22-km grid provide initial conditions for MM5. Presumably, then, errors from the incorrect specification of ini-

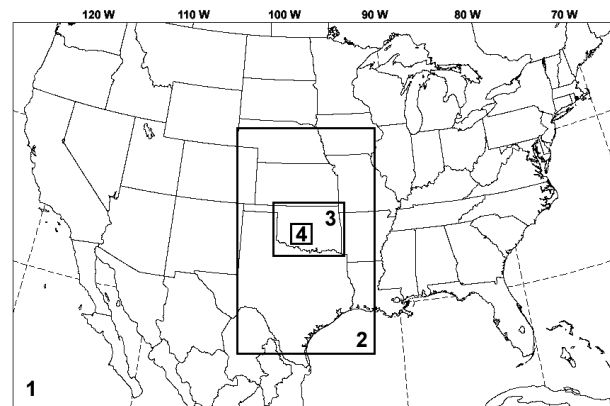


FIG. 1. Location of the four nested MM5 domains with 27-, 9-, 3-, and 1-km resolution.

tial conditions, particularly on scales of 1 km, vastly outweigh the importance of errors introduced by simultaneous derivation of  $\sigma_f$  and LAI.

### 3. METHOD

The primary study area focused on Oklahoma due to the availability of Oklahoma Mesonet observations for soil measurements and model verification. MM5 produced 48-hour forecasts on four nested model domains with 27-, 9-, 3-, and 1-km resolution (Fig. 1) and 23 vertical levels. National Centers for Environmental Prediction (NCEP) Eta model analyses initialized the MM5 forecasts and Eta model forecasts provided boundary conditions every six hours. Specific user-defined options included the Kain and Fritsch (1993) cumulus parameterization on domains 1 and 2 only, the Medium-Range Forecast model (MRF) PBL parameterization (Hong and Pan 1996), simple ice microphysics (Dudhia 1989), and the Rapid Radiative Transfer Model (RRTM) longwave radiation scheme (Mlawer et al. 1997). The Oregon State University land surface model (OSULSM) was chosen as the multi-layer soil model because it is very similar to the land surface model used in the operational Eta model and should facilitate the initialization of soil moisture in MM5 (Chen and Dudhia 2001). Four different initial conditions for the soil and land surface are used to explore the importance of the land surface on the model forecasts.

The control MM5 (CNTRL) uses a climatological  $\sigma_f$ , assumed valid in the middle of each of the 12 months of the year, produced from a 5-year climatology of NDVI observations (Gutman and Ignatov 1998). Values of  $\sigma_f$  at each grid point are temporally interpolated according to the day of the month for each model run. The model also assumes a constant LAI (the default is set to 4.0), regardless of the season or location.

The second MM5 (MM5VEG) initial condition includes the 1-km resolution  $\sigma_f$  and LAI observations derived from a 15-day NDVI composite. These data are interpolated to all four nested model domains. Pixel values within a grid square are averaged to obtain a final value at the center of each grid square (the cross point). A modified MM5 accepts an array of LAI values at cross points for all domains. Satellite-derived  $\sigma_f$  and LAI data cover a swath similar to the area of domain 2. LAI values for cross points outside the area of the satellite pass in domains 1 and 2 are set to a constant 4.0.

The third MM5 (MM5SOIL) initial condition uses Mesonet soil data, but climatology for the vegetation. A two-pass Barnes analysis (Barnes 1973) yields fields of observed soil temperature at depths of 5, 10, and 30 cm beneath native vegetation and soil moisture at 5, 25, and 60 cm depth on MM5 model domains 3 and 4. The analyses are optimized to produce a large response for mesoscale waves, but to damp unrealistic high frequency waves across Oklahoma. Measurements of soil temperature and moisture from the Oklahoma Mesonet replace initial Eta model analyses interpolated to each nested MM5 domain. Two of the four initial soil temperature layers are modified in MM5. The Mesonet observations of soil temperature at a depth of 5 cm replace the initial model soil temperature in the 0–10 cm layer. The second model layer is the layer average temperature from 10–40 cm. To maintain consistency with soil temperatures in the deeper model layers, a cubic spline interpolation is fit between all three observed soil temperatures and the initial model soil temperature in the 40–100 cm layer. The 40–100 cm layer temperature is assumed valid at a depth of 70 cm. The interpolated value at a depth of 25 cm replaces the initial MM5 soil temperature in the 10–40 cm layer. The observed volumetric water content at a depth of 5 cm from the Mesonet replaces the initial

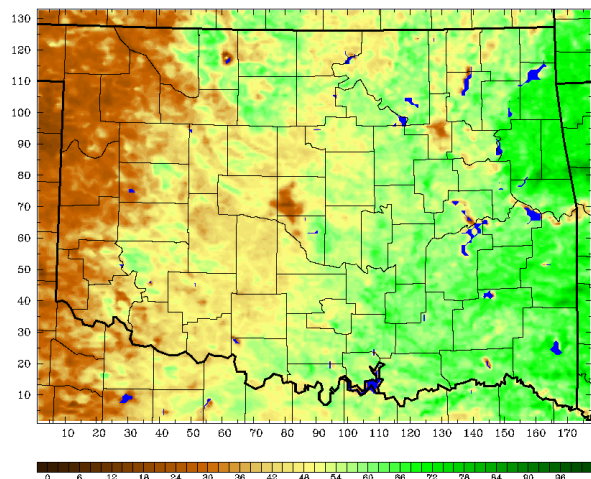


FIG. 2. Fractional vegetation coverage (percentage) for domain 3 calculated from a maximum NDVI composite over the period 1–15 May 2004. Blue areas indicate water bodies.

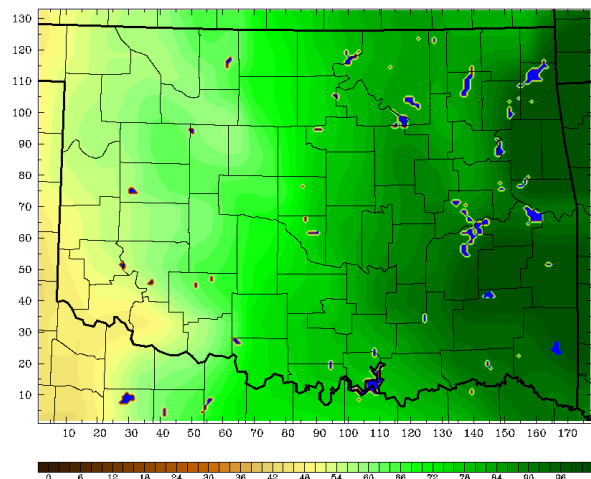


FIG. 3. 17 May 2004 fractional vegetation coverage (percentage) for domain 3 based on a 5-year climatology. Blue areas indicate water bodies.

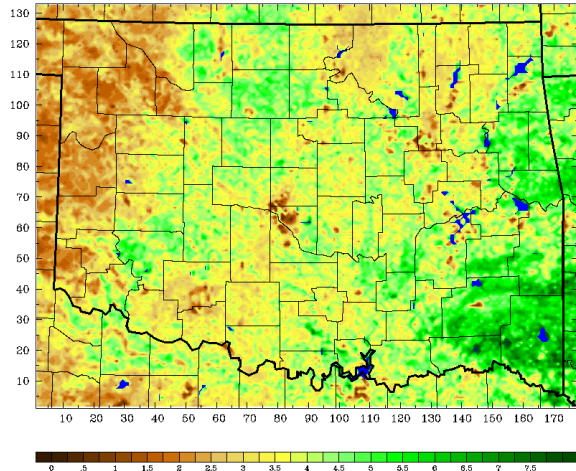


FIG. 4. Leaf area index (dimensionless) for domain 3 calculated from a maximum NDVI composite over the period 1–15 May 2004. Blue areas indicate water bodies.

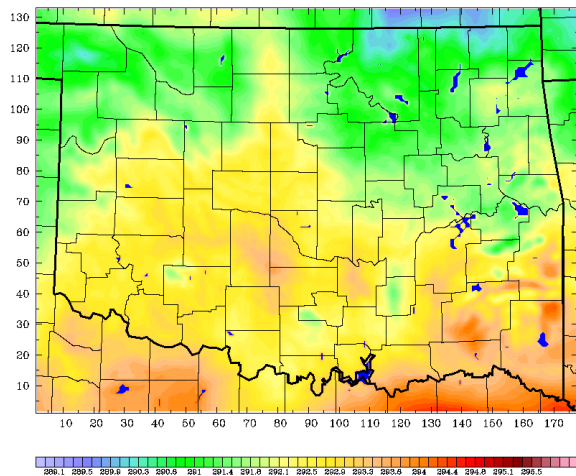


FIG. 5. Initial soil temperature (K) in the 0–10 cm layer for the domain 3 control forecast.

soil moisture field in the 0–10 cm model layer. The 25 cm volumetric water content measurements replace the initial soil moisture field in the 10–40 cm model layer, and the 60 cm volumetric water content measurements replace the initial soil moisture field in the 40–100 cm model layer. The initial soil temperature field in the 40–100 cm layer and both the soil temperature and moisture fields in the 100–200 cm layer remain unchanged from the interpolated Eta analysis for domains 3 and 4. All soil fields for domains 1 and 2 also remain unchanged from the interpolated Eta analysis.

The fourth MM5 (MM5VEGSOIL) initial condition uses the 1-km AVHRR-derived  $\sigma_f$  and LAI values along with the soil data from the Oklahoma Mesonet. This initial condition provides the most accurate specification of the land surface and soil conditions for the model.

An unchanged version of MM5 computed daily 48-

hour forecasts initialized by 1200 UTC Eta analyses during the period 1 April–30 September 2004. Results from 9-, 24-, and 33-hour forecasts of 2-m air temperature and mixing ratio on domain 3 for each model run were compared with corresponding Mesonet observations. This procedure highlighted several good and bad forecasts for further study. For selected cases, the four MM5 initial land surface and soil conditions are used with the same atmospheric initial and boundary conditions to produce 48-hour forecasts. Results from all four types of forecasts are compared with Mesonet observations by interpolating model forecasts to Mesonet station locations.

#### 4. RESULTS

Based on the comparison of daily control forecasts with Mesonet observations, the model forecast initialized

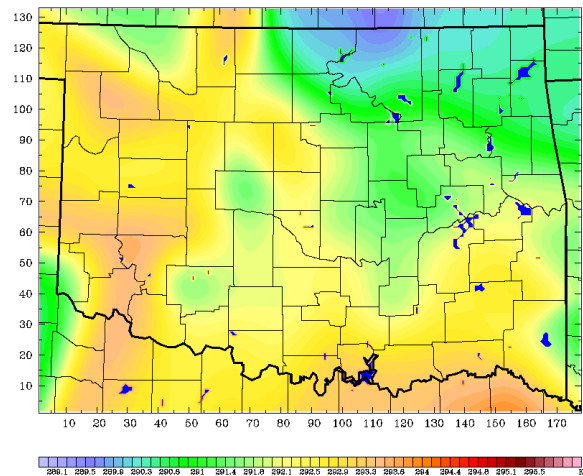


FIG. 6. Initial soil temperature (K) in the 0–10 cm layer analyzed from Oklahoma Mesonet observations for domain 3.

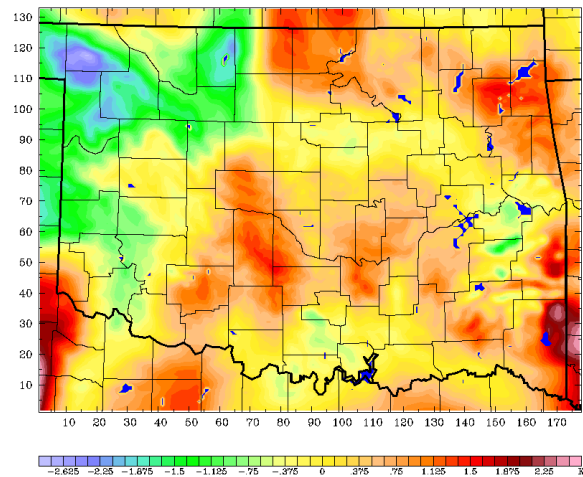


FIG. 7. Difference in initial soil temperature (K) in the 0–10 cm layer after subtracting 1200 UTC analyzed observations from the initial control forecast field.

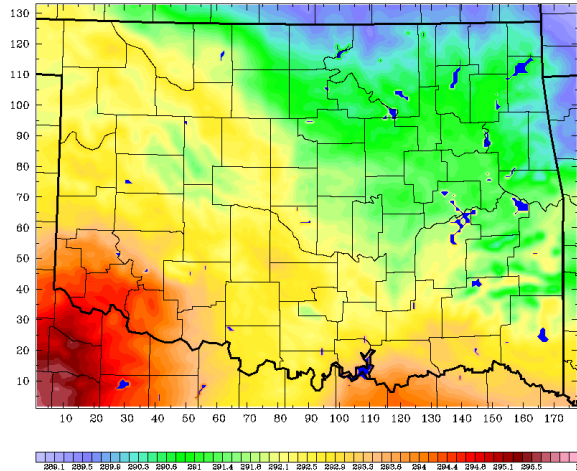


FIG. 8. Initial soil temperature (K) in the 10–40 cm layer for the domain 3 control forecast.

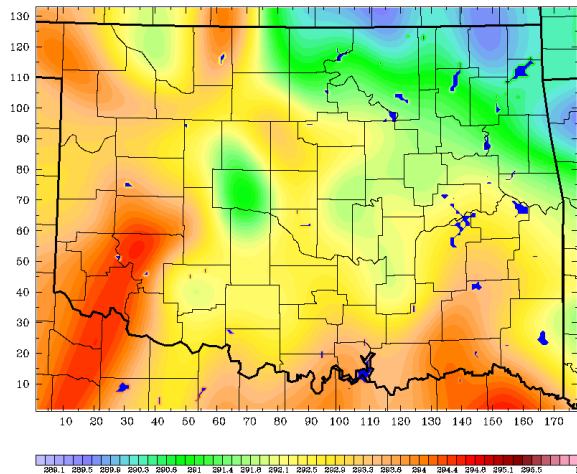


FIG. 9. Initial soil temperature (K) in the 10–40 cm layer analyzed from Oklahoma Mesonet observations for domain 3.

at 1200 UTC 17 May 2004 was selected for further study. The 2-m air temperatures exhibited a warm bias of several degrees Celsius across domain 3 at forecast hours 9 and 33 (late afternoon) and a cool bias at forecast hour 24 (early morning). The model also exhibited a dry 2-m mixing ratio bias at these times. No precipitation fell across domain 3 during the 48-hour forecast period except 3 mm on the morning of 17 May at a Mesonet station in the extreme southeast corner of the domain and 2 mm on 18 May at a single station in extreme northern Oklahoma. Clouds moved across the region during the forecast period, particularly over eastern Oklahoma, but a strong cap prevented widespread convection. Strong southerly winds crossed the state in advance of an approaching cold front and a dryline existed in the Texas Panhandle, but no strong synoptic features passed over domain 3. The poor control forecast under synoptically quiescent conditions makes this an ideal case for study-

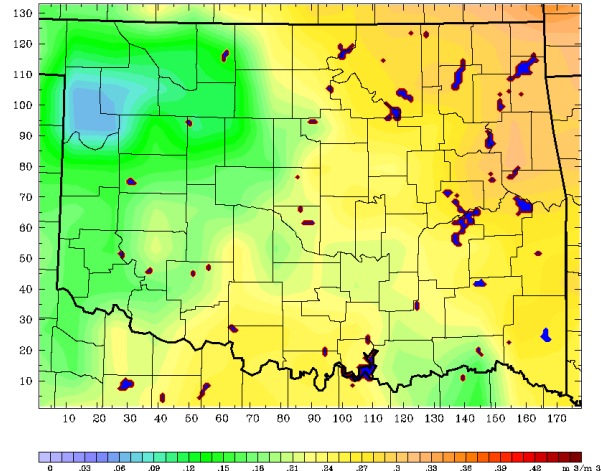


FIG. 10. Initial soil moisture ( $\text{m}^3 \text{m}^{-3}$ ) in the 0–10 cm layer for the domain 3 control forecast.

ing the impact of improved initial conditions on forecasts of radiative fluxes and maximizes the potential for isolating the effect of the land surface model on near-surface atmospheric variables.

The four MM5 forecasts were initialized at 1200 UTC on 17 May 2004 using an Eta analysis interpolated to all four model domains. LAI and  $\sigma_f$  derived from a 15-day maximum NDVI composite over the period 1–15 May 2004 illustrate the stark contrast between observed (Fig. 2) and climatological (Fig. 3)  $\sigma_f$  values for this time period. In addition, the LAI ranges from near 1.0 in western Oklahoma and urban areas to greater than 7.0 in the forests of southeastern Oklahoma (Fig. 4). This information is clearly lost when MM5 employs a constant LAI in control forecasts. MM5SOIL included climatological  $\sigma_f$ , constant LAI, and soil temperature and moisture observations at 1200 UTC on 17 May 2004 from the Oklahoma Mesonet. Initial soil temperatures in the 0–10 cm layer of CNTRL (Fig. 5) and MM5SOIL (Fig. 6) differ by several Kelvin in some locations (Fig. 7). Differences on the order of several Kelvin also appear between the initial soil temperatures in the 10–40 cm layer of CNTRL (Fig. 8) and MM5SOIL (Fig. 9). Similarly, large differences exist between the initial soil moisture field in the 0–10 cm layer in CNTRL (Fig. 10) and the initial field in MM5SOIL (Fig. 11). Maximum differences are on the order of 50% of the range of observed values across the domain (Fig. 12). Similar results appear for the initial 10–40 cm layer (Figs. 13 and 14) and 40–100 cm layer (Figs. 15 and 16) soil moisture fields for both forecasts. MM5VEGSOIL included both satellite observations and soil temperature and moisture observations in the model initialization.

Root-mean-square error (RMSE), mean absolute error (MAE), and bias (Wilks 1995) for forecasts of 2-m air temperature and mixing ratio, 10-meter wind magnitude, and soil temperature and moisture for all of domain 3 illustrate the performance of each forecast. Errors are

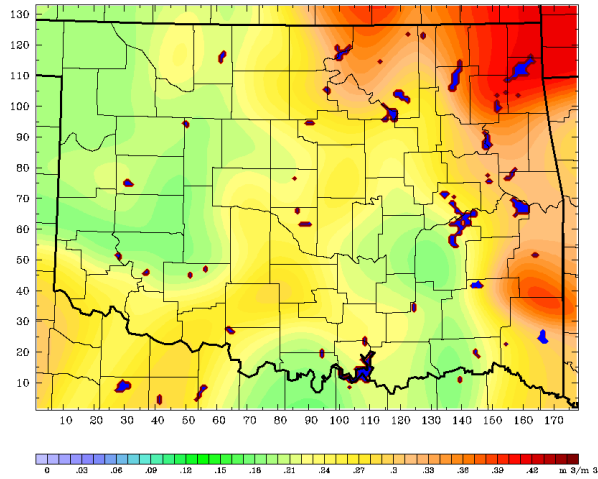


FIG. 11. Initial soil moisture ( $\text{m}^3 \text{m}^{-3}$ ) in the 0–10 cm layer analyzed from Oklahoma Mesonet observations for domain 3.

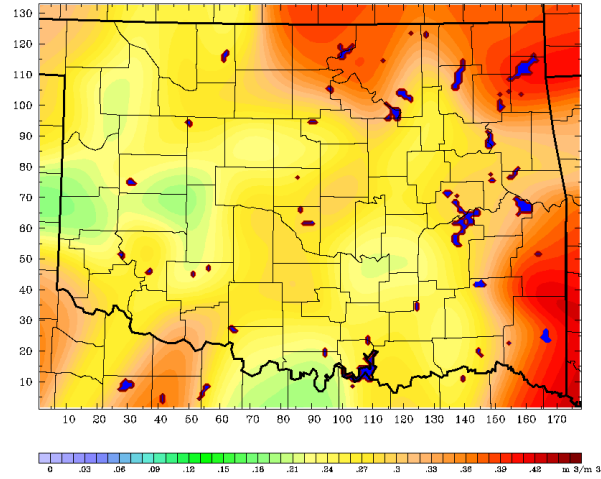


FIG. 14. Initial soil moisture ( $\text{m}^3 \text{m}^{-3}$ ) in the 10–40 cm layer analyzed from Oklahoma Mesonet observations for domain 3.

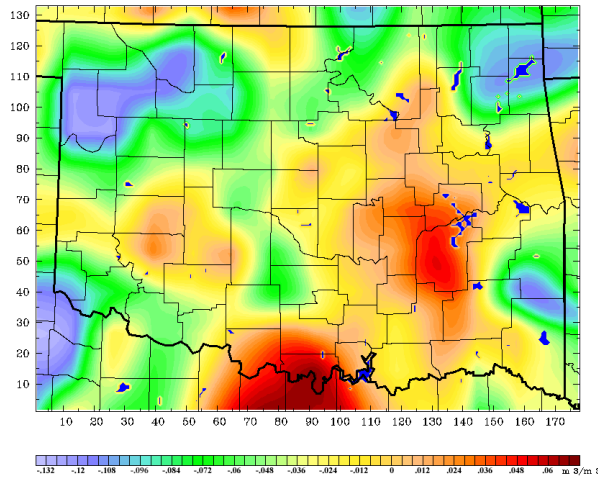


FIG. 12. Difference in initial soil moisture ( $\text{m}^3 \text{m}^{-3}$ ) in the 0–10 cm layer after subtracting 1200 UTC analyzed observations from the initial control forecast field.

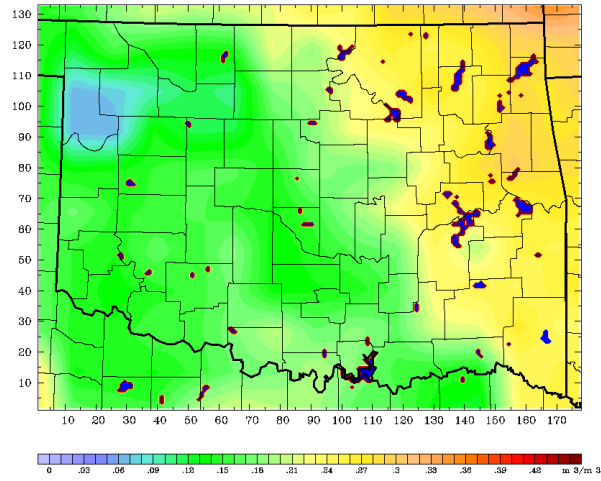


FIG. 15. Initial soil moisture ( $\text{m}^3 \text{m}^{-3}$ ) in the 40–100 cm layer for the domain 3 control forecast.

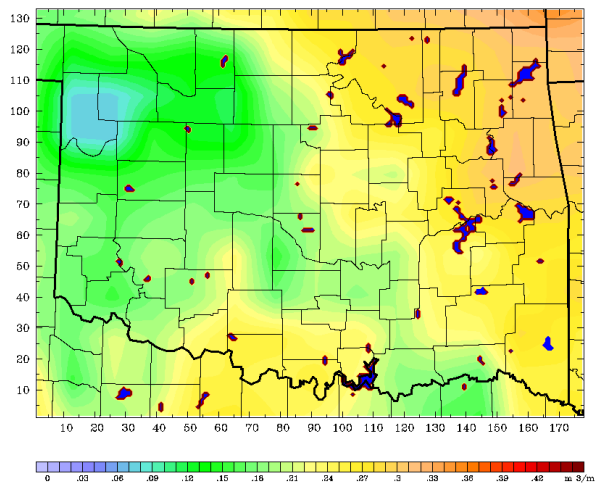


FIG. 13. Initial soil moisture ( $\text{m}^3 \text{m}^{-3}$ ) in the 10–40 cm layer for the domain 3 control forecast.

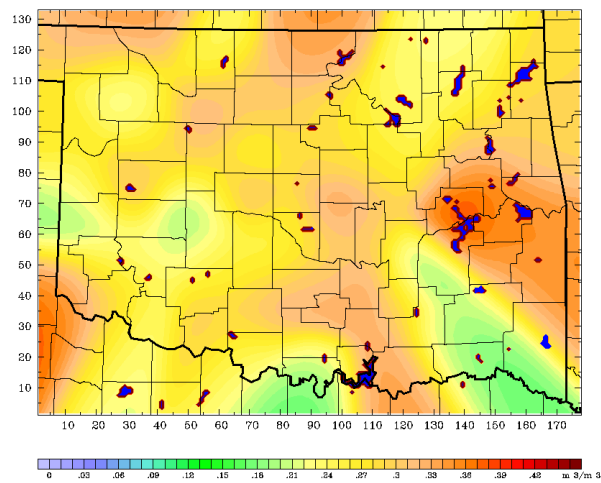


FIG. 16. Initial soil moisture ( $\text{m}^3 \text{m}^{-3}$ ) in the 40–100 cm layer analyzed from Oklahoma Mesonet observations for domain 3.

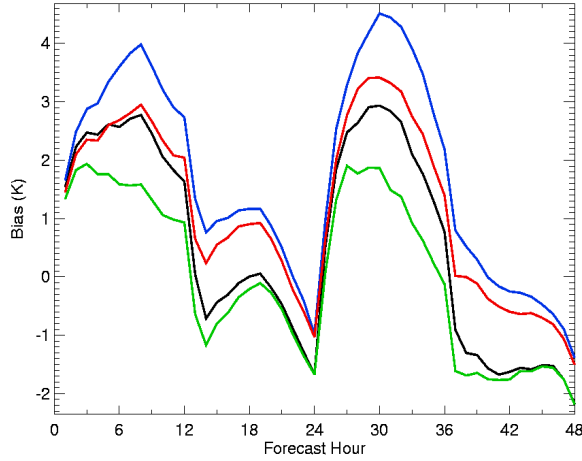


FIG. 17. 2-m air temperature bias (K) after comparison with Oklahoma Mesonet observations in domain 3 for control (black), MM5VEG (blue), MM5SOIL (green), and MM5VEGSOIL (red) forecasts initialized at 1200 UTC 17 May 2004.

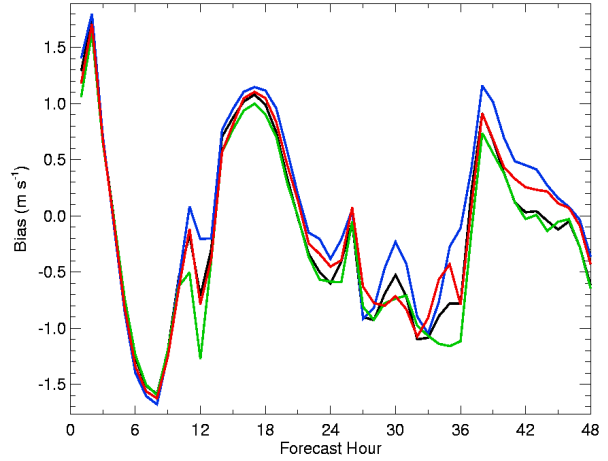


FIG. 19. 10-m wind magnitude bias ( $\text{m s}^{-1}$ ) after comparison with Oklahoma Mesonet observations in domain 3 for control (black), MM5VEG (blue), MM5SOIL (green), and MM5VEGSOIL (red) forecasts initialized at 1200 UTC 17 May 2004.

based on observations from no fewer than 108, 99, and 53 Mesonet sites within domain 3 for atmospheric variables, soil temperature, and soil moisture, respectively. Forecast errors for domain 3 are very similar and representative of the forecast errors for domain 4. MM5SOIL generally produced the best results, reducing bias errors for temperature and mixing ratio forecasts during the day (Figs. 17 and 18). The unrealistic spike in mixing ratio errors around sunset (forecast hours 12 and 36) appears to be an artifact of the interpolation of the mixing ratio from the lowest sigma level to 2 m above ground level at a time when the planetary boundary layer undergoes a rapid transition to nighttime stable conditions. All wind magnitude forecasts differed only slightly (Fig. 19). Soil temperature (Fig. 20) and soil moisture (Fig. 21) values

were clearly more accurate in MM5SOIL.

Given the marked discrepancy between observed and climatological  $\sigma_f$  and the observed departure from a constant LAI in MM5VEG, and increased initial soil moisture in MM5SOIL, one would expect large changes in latent heat flux in some areas (Fig. 22) compared with CNTRL. The maximum difference between the domain 4 MM5VEG and MM5SOIL forecasts of latent heat flux at Norman, Oklahoma exceeds  $180 \text{ W m}^{-2}$ . Additionally, the maximum difference in sensible heat flux is greater than  $115 \text{ W m}^{-2}$  (Fig. 23). Differences are even larger for lower-resolution domain 3 forecasts. Sensible heat flux bias errors for MM5VEG exceed  $100 \text{ W m}^{-2}$  during the daytime, though MM5SOIL does remarkably well (Fig. 24). Consistent with results from

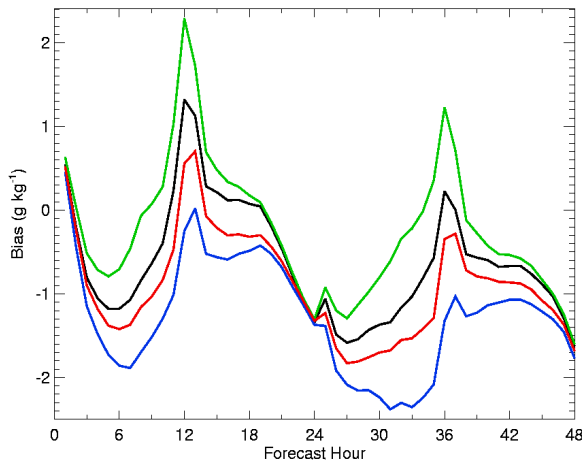


FIG. 18. 2-m mixing ratio bias ( $\text{g kg}^{-1}$ ) after comparison with Oklahoma Mesonet observations in domain 3 for control (black), MM5VEG (blue), MM5SOIL (green), and MM5VEGSOIL (red) forecasts initialized at 1200 UTC 17 May 2004.

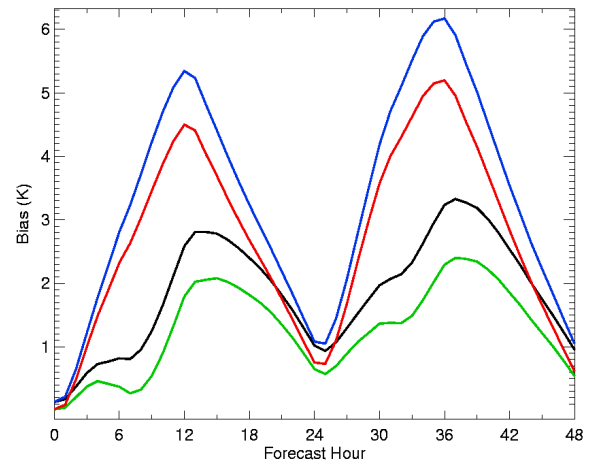


FIG. 20. Soil temperature bias (K) in the 0–10 cm layer after comparison with Oklahoma Mesonet observations in domain 3 for control (black), MM5VEG (blue), MM5SOIL (green), and MM5VEGSOIL (red) forecasts initialized at 1200 UTC 17 May 2004.

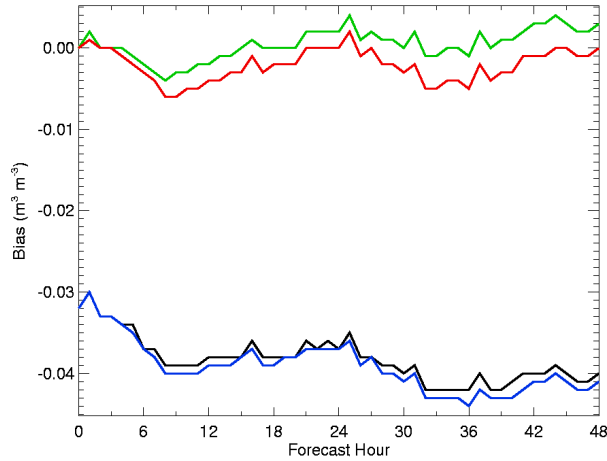


FIG. 21. Soil moisture bias ( $\text{m}^3 \text{m}^{-3}$ ) in the 0–10 cm layer after comparison with Oklahoma Mesonet observations in domain 3 for control (black), MM5VEG (blue), MM5SOIL (green), and MM5VEGSOIL (red) forecasts initialized at 1200 UTC 17 May 2004.

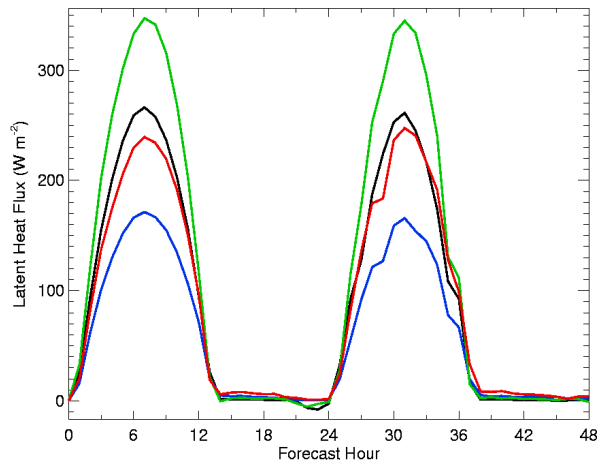


FIG. 22. Latent heat flux ( $\text{W m}^{-2}$ ) at Norman, Oklahoma for control (black), MM5VEG (blue), MM5SOIL (green), and MM5VEGSOIL (red) domain 4 forecasts initialized at 1200 UTC 17 May 2004.

Marshall et al. (2003), both of these factors contribute to lower daytime temperature and mixing ratio bias errors for the MM5SOIL forecast and higher bias errors for the MM5VEG forecast compared with the control forecast. At Norman, these factors result in a maximum temperature difference between the domain 4 MM5SOIL forecast and the MM5VEG forecast of greater than  $3^\circ\text{C}$ , though daily maximum temperatures still exceed observations for all four forecast types (Fig. 25).

All four forecasts consistently overestimated the quantity of incoming shortwave radiation compared with observations under clear skies. This difference between forecasts and observations is probably not a result of dirt and debris covering Mesonet pyranometers, but is perhaps due to a lack of attenuation and absorption by aerosols and ozone in the model radiation scheme. Mar-

shall et al. (2003) discuss similar problems with Eta model simulations. The overestimated shortwave radiation could be overwhelming the effect of changes in the land surface model initial conditions. This illustrates the profound difficulty in evaluating individual model components when all of the schemes are interdependent.

## 5. CONCLUSIONS

Modifications to the initial vegetation and soil fields clearly affect forecasts produced by the OSULSM. Large discrepancies exist between climatological  $\sigma_f$  and observed  $\sigma_f$  derived from a fifteen-day maximum NDVI composite. Initial soil moisture fields initialized by the Eta model are generally too dry, while soil temperature

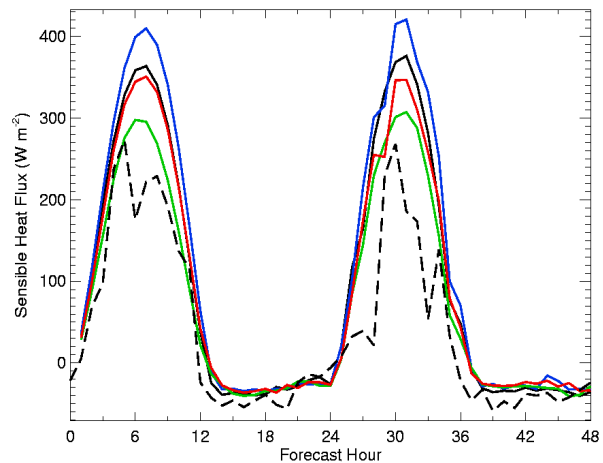


FIG. 23. Sensible heat flux ( $\text{W m}^{-2}$ ) at Norman, Oklahoma for control (black), MM5VEG (blue), MM5SOIL (green), and MM5VEGSOIL (red) domain 4 forecasts initialized at 1200 UTC 17 May 2004, and corresponding observations (dashed).

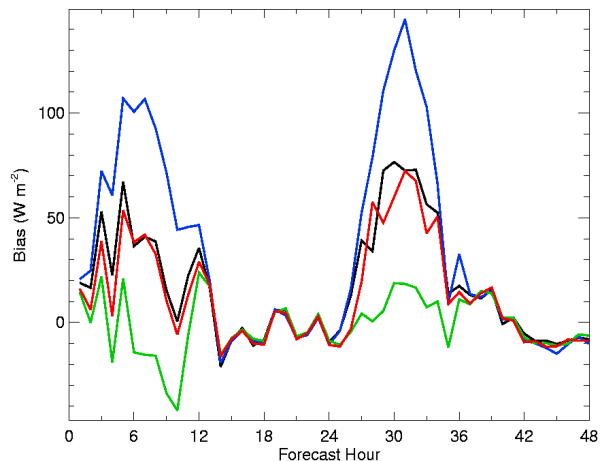


FIG. 24. Sensible heat flux bias ( $\text{W m}^{-2}$ ) after comparison with Oklahoma Mesonet observations in domain 3 for control (black), MM5VEG (blue), MM5SOIL (green), and MM5VEGSOIL (red) forecasts initialized at 1200 UTC 17 May 2004.

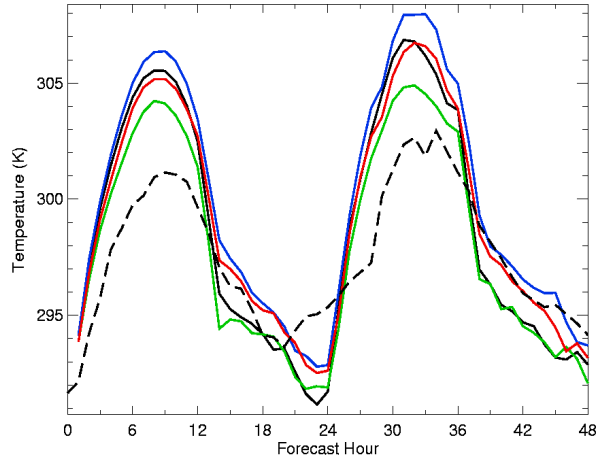


FIG. 25. 2-m air temperature (K) at Norman, Oklahoma for control (black), MM5VEG (blue), MM5SOIL (green), and MM5VEGSOIL (red) domain 4 forecasts initialized at 1200 UTC 17 May 2004, and corresponding observations (dashed).

fields are within a few degrees Celsius of the observations. Despite using 40–100 cm layer soil temperatures interpolated from Eta analyses to assign 10–40 cm layer soil temperatures, these differences in soil temperature and moisture persist throughout the entire forecast period. The model, however, does add small-scale gradients to the soil temperature and moisture fields by accounting for differences in land use and soil type. The overall MM5SOIL forecast and MM5VEGSOIL forecast bias errors for soil temperature and moisture do not drift appreciably back to control forecast errors during the forecast period. These differences in initial conditions cause planetary boundary layer heights over the forecast period to differ between the four forecast types by more than 1000 m in some areas. However, errors in incoming shortwave radiation may offset the benefits of improved land surface initial conditions.

Only the MM5SOIL forecast showed considerable improvement over the control forecast. Forecast errors for most variables were reduced when verified with observations from the Oklahoma Mesonet. Forecasts incorporating satellite-derived vegetation indices into the initial conditions, however, generally produced worse results than the control forecast. The OSULSM may be tuned to provide the best results for a constant LAI. Further studies will focus on maintaining a constant LAI and modifying only  $\sigma_f$ . The MM5VEGSOIL forecast partially compensated for surface energy flux errors in the MM5VEG forecast by improving the initial soil temperature and moisture fields.

These results stress the significance of minimizing errors in surface initial conditions. Accurate soil measurements in particular have a lasting impact on model forecasts. While the effect of initial atmospheric fields is certainly important for short-term forecasts, soil temperature and moisture fields may impact local weather for

several days. Realistic specification of these fields can significantly improve forecast accuracy.

Operational forecasts that assimilate improved land surface conditions will require additional data. Modernized synoptic observations should include soil measurements in order to minimize surface initial conditions on a larger scale. The Earth Observing System (EOS) Moderate-Resolution Imaging Spectroradiometer (MODIS) is still experimental and has an uncertain future. However, this satellite provides daily coverage in 36 spectral bands at 250–100-m resolution (Justice et al. 1998) and would provide even higher resolution vegetation information than presently available from AVHRR measurements.

Further studies will refine the data assimilation process to maximize the accuracy of initial surface conditions. In particular, a reduced time window for calculating maximum NDVI composites and a moving time window ending within 24 hours of the model initialization time would produce more representative initial  $\sigma_f$  and LAI values. Assimilation of more Oklahoma Mesonet observations, including surface fluxes and atmospheric variables, would likely improve model forecasts.

*Acknowledgments.* The authors wish to thank Dr. James Merchant and Roberto Bonifaz of the University of Nebraska–Lincoln School of Natural Resource Sciences for providing fractional vegetation coverage and leaf area index data. Funding was provided under NSF grant ATM-0243720.

## REFERENCES

- Barnes, S.L., 1973: Mesoscale objective analysis using weighted time-series observations. NOAA Tech. Memo. ERL NSSL-62, National Severe Storms Laboratory, Norman, OK 73069, 60 pp. [NTIS COM-73-10781].
- Basara, J.B., and T.M. Crawford, 2000: Improved installation procedures for deep-layer soil moisture measurements. *J. Atmos. Oceanic Technol.*, **17**, 879–884.
- Brock, F.V., K.C. Crawford, R.L. Elliot, G.W. Cuperus, S.J. Stadler, H.L. Johnson, and M.D. Eilts, 1995: The Oklahoma Mesonet: A technical overview. *J. Atmos. Oceanic Technol.*, **12**, 5–19.
- Chang, J.-T., and P.J. Wetzel, 1991: Effects of spatial variations of soil moisture and vegetation on the evolution of a prestorm environment: A numerical case study. *Mon. Wea. Rev.*, **119**, 1368–1390.
- Chen, F., and J. Dudhia, 2001: Coupling an advanced land surface – hydrology model with the Penn State–NCAR MM5 modeling system. Part I: Model implementation and sensitivity. *Mon. Wea. Rev.*, **129**, 569–585.
- , K. Mitchell, J. Schaake, Y. Xue, H.-L. Pan, V. Koren, Q.Y. Duan, M. Ek, and A. Betts, 1996: Modeling of land-surface evaporation by four schemes and comparison with FIFE observations. *J. Geophys. Res.*, **101**, 7251–7268.
- Crawford, T.M., D.J. Stensrud, T.N. Carlson, and W.J. Capehart, 2000: Using a soil hydrology model to obtain regionally averaged soil moisture values. *J. Hydrometeorol.*, **1**, 353–363.

- , —, F. Mora, J.W. Merchant, and P.J. Wetzel, 2001: Value of incorporating satellite-derived land cover data in MM5/PLACE for simulating surface temperatures. *J. Hydrometeor.*, **2**, 453–468.
- Dudhia, J., 1989: Numerical study of convection observed during the Winter Monsoon Experiment using a mesoscale two-dimensional model. *J. Atmos. Sci.*, **46**, 3077–3107.
- , 1993: A nonhydrostatic version of the Penn State–NCAR mesoscale model: Validation tests and simulation of an Atlantic cyclone and cold front. *Mon. Wea. Rev.*, **121**, 1493–1513.
- , 1996: A multi-layer soil temperature model for MM5. Preprints, *Sixth PSU/NCAR Mesonet Model Users' Workshop*, Boulder, CO, PSU/NCAR, 49–50.
- Goodrum, G., K.B. Kidwell, and W. Winston, 2001: NOAA KLM User's Guide, National Oceanic and Atmospheric Administration, Silver Spring, MD.
- Grell, G.A., J. Dudhia, and D.R. Stauffer, 1994: A description of the fifth-generation Penn State/NCAR Mesoscale Model (MM5). NCAR/TN-398+STR, 121 pp. [Available from MMM Division, NCAR, P.O. Box 3000, Boulder, CO 80307.]
- Gutman, G., and A. Ignatov, 1998: The derivation of the green vegetation fraction from NOAA/AVHRR data for use in numerical weather prediction models. *Int. J. Remote Sens.*, **19**, 1533–1543.
- , D. Tarpley, A. Ignatov, and S. Olson, 1995: The enhanced NOAA global land dataset from the Advanced Very High Resolution Radiometer. *Bull. Amer. Meteor. Soc.*, **76**, 1141–1156.
- Hong, S.-Y., and H.-L. Pan, 1996: Nonlocal boundary layer vertical diffusion in a medium-range forecast model. *Mon. Wea. Rev.*, **124**, 2322–2339.
- Justice, C.O., and Coauthors, 1998: The moderate resolution imaging spectroradiometer (MODIS): Land remote sensing for global change research. *IEEE Trans. Geosci. Remote Sens.*, **36**, 1228–1249.
- Kain, J.S., and J.M. Fritsch, 1993: Convective parameterization for mesoscale models: The Kain–Fritsch scheme. *The Representation of Cumulus Convection in Numerical Models*, Meteor. Monogr., No. 46, Amer. Meteor. Soc., 165–170.
- Kidwell, K.B., 1998: NOAA Polar Orbiter Data User's Guide, U.S. Department of Commerce, NESDIS, NOAA, National Climatic Data Center, Satellite Data Services Division, Washington, D.C.
- Kurkowski, N.P., D.J. Stensrud, and M.E. Baldwin, 2003: Assessment of implementing satellite-derived land cover data in the Eta model. *Wea. Forecasting*, **18**, 404–416.
- Marshall, C.H., K.C. Crawford, K.E. Mitchell, and D.J. Stensrud, 2003: The impact of the land surface physics in the operational NCEP Eta model on simulating the diurnal cycle: Evaluation and testing using Oklahoma Mesonet data. *Wea. Forecasting*, **18**, 748–768.
- Mlawer, E.J., S.J. Taubman, P.D. Brown, M.J. Iacono, and S.A. Clough, 1997: Radiative transfer for inhomogeneous atmospheres: RRTM, a validated correlated-k model for the longwave. *J. Geophys. Res.*, **102**, 16 663–16 682.
- Oleson, K.W., and G.B. Bonan, 2000: The effects of remotely sensed plant functional type and leaf area index on simulations of boreal forest surface fluxes by the NCAR land surface model. *J. Hydrometeor.*, **1**, 431–446.
- Scurlock, J.M.O., G.P. Asner, and S.T. Gower, 2001: Worldwide historical estimates of leaf area index, 1932–2000. Technical Memorandum ORNL/TM-2001/268. Oak Ridge National Laboratory, Oak Ridge, TN, 40 pp.
- Shafer, M.A., C.A. Fiebrich, D.S. Arndt, S.E. Fredrickson, and T.W. Hughes, 2000: Quality assurance procedures in the Oklahoma Mesonet network. *J. Atmos. Sci.*, **17**, 474–494.
- Viña, A., G.M. Henebry, and A.A. Gitelson, 2004: Satellite monitoring of vegetation dynamics: Sensitivity enhancement by the wide dynamic range vegetation index. *Geophys. Res. Lett.*, **31**, L04503, doi:10.1029/2003GL019034.
- Wilks, D.S., 1995: *Statistical Methods in the Atmospheric Sciences*. International Geophysics Series, Vol. 59, Academic Press, 464 pp.
- Zeng, X., R.E. Dickinson, A. Walker, M. Shaikh, R.S. DeFries, and J. Qi, 2000: Derivation and evaluation of global 1-km fractional vegetation cover data for land modeling. *J. Appl. Meteor.*, **39**, 826–839.
- Zhangshi, Y., and T.H.L. Williams, 1997: Obtaining spatial and temporal vegetation data from Landsat MSS and AVHRR/NOAA satellite images for a hydrological model. *Photogr. Eng. Remote Sens.*, **63**, 69–77.